Neuronatin mediated aberrant calcium signaling and endoplasmic reticulum stress underlie neuropathology in Lafora disease

Jaiprakash Sharma[1], Diptendu Mukherjee[1], Sudheendra N. R. Rao[1], Saumya Iyenger[2], Susarla Krishna Shankar[3], Parthasarathy Satishchandra[4], and Nihar Ranjan Jana[1,*]

From the [1]Cellular and Molecular Neuroscience and [2]Neuroanatomy Laboratory, National Brain Research Centre, Manesar, Gurgaon - 122 050, India; Department of [3]Neuropathology and [4]Neurology, National Institute of Mental Health and Neurosciences, Bangalore, India.

Running title: Neuronatin in Lafora disease pathogenesis

*Address correspondence to: Nihar Ranjan Jana, Cellular and Molecular Neuroscience Laboratory, National Brain Research Centre, Manesar, Gurgaon - 122 050, India. Tel: +91-124-2815217, Fax: +91-124-2338910, e-mail: nihar@nbrc.ac.in

Capsule:
Background: Neuronatin was identified as a novel substrate of Lafora disease ubiquitin ligase malin, however, its role in disease biology is unknown.
Results: Neuronatin causes increased intracellular Ca^{+2} and ER stress and accumulated as insoluble aggregates in LD brain and skin biopsy samples.
Conclusion: Neuronatin-induced aberrant Ca^{+2} signaling might trigger LD pathogenesis.
Significance: These findings provide a new insight in understanding the LD pathogenesis.

Lafora disease (LD) is a teenage onset inherited progressive myoclonus epilepsy characterized by the accumulations of intracellular inclusions called Lafora bodies and caused by mutations in protein phosphatase laforin or ubiquitin ligase malin. But how the loss-of-function of either laforin or malin causes disease pathogenesis is poorly understood. Recently, neuronatin was identified as a novel substrate of malin that regulates glycogen synthesis. Here we demonstrate that the level of neuronatin is significantly up-regulated in the skin biopsy sample of LD patients having mutations in both malin and laforin. Neuronatin is highly expressed in human fetal brain with gradual decrease in expression in adolescent and adult brain. However, in adolescent and adult brain, neuronatin is predominantly expressed in parvalbumin-positive GABAergic interneurons and localize in their processes. The level of neuronatin is increased and accumulated as insoluble aggregates in the cortical areas of LD brain biopsy samples and there is also a dramatic loss of parvalbumin-positive GABAergic interneurons. Ectopic expression of neuronatin in cultured neuronal cells result in increased intracellular Ca^{2+}, endoplasmic reticulum stress, proteasomal dysfunction and cell death that can be partially rescued by malin. These findings suggest that the neuronatin-induced aberrant Ca^{2+} signaling and endoplasmic reticulum stress might underlie LD pathogenesis.

Introduction

Lafora disease (LD) is an autosomal recessive progressive myoclonus epilepsy, usually manifest during teenage and patient dies within a decade of disease onset. The disease is clinically characterized by progressive increase in generalized tonic-clonic seizures, myoclonic and visual seizures, dementia, psychoses, muscles wasting leading the patient to a vegetative state and ultimately death (1-5). Pathological features of LD include gradual increase in accumulation of insoluble polyglucosan bodies (commonly known

as Lafora bodies) and in neuronal loss. Lafora bodies are not only observed in brain but also in other non-neuronal tissues like liver, heart, skeletal muscle, skin etc. (1,3,6).

LD is caused by mutations in the *EPM2A* or *EPM2B* (*NHLRC1*) genes encoding laforin (a protein phosphatase) and malin (a E3 ubiquitin ligase) respectively (2,7-9). Patients with mutations in either laforin or malin are clinically and pathologically indistinguishable (2,10), indicating that both these proteins work together in some common signaling pathways and defect in those pathways could lead to disease manifestation. Emerging evidence indicates that both laforin and malin could play an important role in regulation of glycogen metabolism (11-15), in autophagy (16-18) and in Wnt signaling pathway (19,20). Knockout mice for both laforin and malin also exhibit progressive accumulation of Lafora bodies in various tissues including brain, defects in autophagic degradation pathway and widespread neurodegeneration (17,18,21-24). Current finding in LD mice models point towards the role of abnormal accumulation of Lafora bodies (18,23,25), and impairment of intracellular protein degradation pathways (17,18,26) in the disease pathogenesis. Lafora bodies in the brain are also associated with a number of cellular factors including the components of ubiquitin-proteasome system (UPS) and autophagy indicating further the involvement of these protein degradation pathways in disease progression (17,26). But how exactly Lafora bodies induce neurodegeneration is not clear at present and the possible mechanism of dysfunction of protein degradation pathways in LD is also poorly understood.

Neuronatin, a small proteolipid family membrane protein, is highly expressed in embryonic brain and suggested to be involved in brain development (27,28). It exists in two major isoforms, α and β consisting of 81 and 54 amino acids respectively (29,30). In adult mice brain, it is expressed at very low levels and that also largely restricted to limbic structures (31). Neuronatin is also expressed in several other peripheral tissues including pancreas, adipose tissues and skin (32-34). Although the physiological function of neuronatin is poorly understood, existing literature indicate its involvement in glucose-mediated insulin secretion from pancreas, in adipogenesis and in metabolic regulation (31,32,35-37). Interestingly, neuronatin has significant homology with phospholamban and PMP1 that function as regulatory subunit of ion channel and shown to promote neural lineage in embryonic stem cells through increasing the intracellular Ca^{2+} by antagonizing serco/endoplasmic reticulum Ca^{2+}-ATPase-2 (SERCA2) (27,38). Recently, we have reported that malin interacts with neuronatin and promotes its proteasome-mediated degradation. Malin also negatively regulates neuronatin-stimulated glycogen synthesis (39). Here we demonstrate that neuronatin level is increased in LD skin biopsy samples irrespective of mutation in either malin or laforin and accumulated as insoluble aggregates in LD brain biopsy samples. We also provide evidence that neuronatin-mediated aberrant Ca^{2+} signaling might be an important early event leading to neurodegeneration in LD by inducing ER and proteasomal stress.

Experimental Procedures

Materials—Cell culture media, MG132, N6,2'-O-dibutyryl-adenosine-3',5' cyclic monophosphate(dbcAMP), thapsigargin, tunicamycin and mouse monoclonal calbindin antibody were purchased from Sigma. Lipofectamine® 2000, optiMEM, Fura-2AM and mouse monoclonal V5 antibody were purchased from Invitrogen. Fetal bovine serum and antibiotics penicillin/streptomycin were obtained from GIBCO and Bradford reagent and pre stained protein molecular weight markers were procured from BioRad. Mouse monoclonal anti-myc, anti-GAPDH, anti-CHOP, rabbit polyclonal anti-IRE-α, anti-β-tubulin, and goat polyclonal anti-Hsc70/Hsp70 and anti-Grp78 were purchased from Santa Cruz Biotechnologies. Rabbit polyclonal anti-ubiquitin, mouse monoclonal anti-

GFP and rabbit polyclonal anti-neuronatin were purchased from Dako, Roche and Abcam respectively. Rabbit polyclonal parvalbumin antibody was obtained from Swant. HRP and fluorophore conjugated secondary antibodies, Novared kit and Vectashield mounting media with DAPI were purchased from Vector Laboratories. The construction of malin-V5, neuronatin β-myc plasmid and the source of pd1EGFP and C26S malin plasmids were described elsewhere (39-41). Mouse specific neuronatin siRNA (a pool of 3 target specific 20-25 nucleotide) and control (scramble sequences) were purchased from Santa Cruz Biotechnologies.

The serial paraffin sections of axillary skin and brain biopsy samples, paraffin section of control brain with different ages (39 weeks, 11, 14 and 37 years) were obtained from the archives of Human Brain Tissue Repository, National Institute of Mental Health and Neurosciences, Bangalore, India, according to the ethical guidelines of Indian Council of Medical Research, with consent of the subject to utilize the material for research purposes, protecting the confidentiality of the subject. We used three clinically and genetically confirmed LD (malin mutants; L279P and delF216-D233 and laforin mutant; N148Y) and three normal skin biopsy samples (samples serial no; 1718, 1762 and 1848) in this study. Two clinically confirmed cases of LD brain biopsy samples (LD1, 623; LD2, 544) were used in our study. LD1 and LD2 patients were of 17 and 23 years old respectively.

Cell culture, transfection and immunoblotting—Neuro 2a cells were routinely cultured in DMEM with 10% fetal bovine serum and antibiotics penicillin/streptomycin. Cells were plated at sub confluent density into 6-well tissue cultured plates and transfected after 24 h with Lipofectamine® 2000 according to the manufacturer's instruction. Transfection efficiency was approximately 50-60%. After 36 or 48 h of transfection, cells were collected, washed twice in ice cold PBS, pelleted by centrifugation and lysed under ice for 30 min using Nonident P-40 (NP-40) lysis buffer (50 mM Tris; pH 8.0, 150 mM NaCl, 1% NP-40, complete EDTA-free protease inhibitor cocktail). Cell lysates were collected after brief sonication and centrifugation at 20,000xg for 15 min. Protein concentrations were measured using Bradford method. Total cell lysates were resolved through SDS-polyacrylamide gel electrophoresis and processed for immunoblotting as described elsewhere (42). Neuronatin and V5 antibody were used at 1:5000 dilutions; myc, IRE-α, Grp78, CHOP, ubiquitin and β-tubulin antibody at 1:1000 dilutions; GAPDH at 1:15,000 dilutions.

Immunofluorescence staining and counting of apoptotic cells—Neuro 2a cells grown in 2-well tissue cultured chamber slides were transiently transfected with various plasmids, differentiated with dbcAMP and 72 h of post transfection, cells were processed for immunofluorescence staining. In some experiment cells were treated with MG132 and subjected to immunofluorescence staining. Briefly, cells were washed in PBS thrice, fixed with 4% Paraformaldehyde in PBS for 30 minutes. After fixation, cell were washed thrice again with PBS and permeabilized with 0.3 % TritonX-100 in PBS for 10 min and subsequently blocked with 3% BSA in PBS for 1 h. Cells were incubated with various primary antibodies overnight at 4^{o}C. After three washings with PBS, cells were incubated with fluorophore-conjugated secondary antibody for 1 h. Cells were finally washed with PBS and mounted in mounting media containing DAPI and imaged using Axioplan fluorescence microscope/Apotome (Zeiss). Anti-myc, anti-neuronatin and anti-V5 were used at 1:1000 dilutions.

Transfected cells exhibiting apoptotic bodies (fragmented nuclei) were manually counted at 20X magnification. Fields were randomly selected and approximately 200 cells were scored per experiment. Each experiment was repeated at least 3 times and counts were performed in a blinded manner.

Measurement of intracellular Ca^{2+} level—Neuro 2a cells were plated into 6 well tissue culture

plates and transfected with various plasmids and neuronatin siRNA. 1μM thapsigargin was added in one of the wells for 12 h to serve as the positive control. Thirty-six hours of post transfection, cells were washed with PBS, and loaded with 5 μM Fura-2AM for 30 min. Cells were then washed and treated with 1X HBSS for 45 min, washed, collected and transferred to a 96-well black bottom plate and the fluorescence was measured using a fluorescence plate reader having an excitation filter of 340 and 380 nm and an emission filter of 510 nm. The raw data was obtained and the intracellular calcium concentration was calculated from the ratio (R) of fluorescence emissions (F) at excitation wavelengths of 340 and 380 nm (F340/F380) according to the equation described earlier (43).

Immunohistochemical techniques and PAS staining—The paraffin embedded axillary skin and brain sections were deparaffinized with xylene, rehydrated with gradually decreasing percent of alcohol and subjected to antigen retrieval in a pressure cooker. The sections were treated with 3% H_2O_2 in methanol, permeabilized in 0.3% Triton X-100, blocked with 5% goat serum containing 0.1% Triton X-100. The sections were incubated with primary antibodies to neuronatin (1:1000 dilutions), ubiquitin (1:200 dilutions) and Hsc70/Hsp70 (1:250 dilutions), respectively for overnight. Color development was carried out using the Nova red kit. One section from each case was subjected to PAS staining to confirm the presence of Lafora bodies according to previously described method (44). In some experiment, control human brain section was subjected to double immunofluorescence staining using either parvalbumin and neuronatin antibodies or neuronatin and calbindin antibodies.

Proteasome activity assays—Neuro 2a cells were seeded onto 6-well tissue cultured plates and after overnight of platting cells were transfected with various plasmids and treated with dbcAMP. Collected cells were processed for proteasome activity assays as previously described (41). The substrates Suc-Leu-Leu-Val-Tyr-MCA and Z-Leu-Leu-Glu-MCA were used to measure the chymotrypsin-like and post-glutamyl peptidyl hydrolytic-like protease activity respectively.

Statistical Analysis—Data were analyzed by one-way analysis of variance using SigmaStat software. Values were presented as mean ± SD. The Bonferroni post hoc test was conducted to compare individual means where analysis of variance indicated statistical differences. $P<0.05$ was considered statistically significant.

Results

Skin biopsy samples of LD patients having mutations in either laforin or malin exhibit increased level of neuronatin—We have recently identified neuronatin as a novel interacting partner of malin. Malin induces ubiquitination and proteasome-mediated degradation of neuronatin (39). We further explored the significance of interaction of malin with neuronatin in the context of LD pathogenesis. First, we studied and compared the level of neuronatin in skin biopsy sample of LD patients along with age-matched control subjects. It is important to note that the Lafora bodies are frequently observed in the apocrine sweat gland of skin (34) and skin biopsies are routinely carried out to diagnose LD (1). Since neuronatin is abundantly expressed in sweat gland of human skin, we took the advantage of easily accessible LD skin biopsy samples to study the level of neuronatin. In control subject, neuronatin was expressed in myoepithelial cells of the sweat glands and localized mostly in the membrane with diffuse cytoplasmic staining pattern. However, in the malin mutants LD skin biopsy sample, neuronatin staining was strongly increased not only in the membrane and cytoplasm but also in the nucleus of the myoepithelial cells of sweat gland (Fig.1). Similar increase and redistribution of neuronatin into the nucleus was also detected in the LD skin biopsy samples having laforin mutation. These finding suggests that functional laforin-malin complex

might be essential in the regulation of neuronatin level.

Age-dependent expression and localization of neuronatin in human brain—Our next goal was to characterize the expression of neuronatin in the LD brain and its involvement in LD pathogenesis. Neuronatin expression is developmentally regulated in rodent brain. However its expression pattern and localization in human brain is not well known. Therefore, we next attempted to study the expression and localization of neuronatin in human brain with different ages. Figure 2A showed that the expression of neuronatin is very high in the cortical area of 39 weeks old brain. However its expression was drastically reduced in the cortex of 15 and 50 years old brain (see also supplementary Fig.S1). Interestingly, a selective population of neurons expressed high level of neuronatin and it was localized not only in the cell soma but also in the neuronal processing. Further search revealed that the parvalbumin-positive (PV+ve) GABAergic interneurons selectively expressed high levels of neuronatin in the brains of 15 and 50 years old individuals (Fig.2B), while neuronatin was not expressed in calbindin-positive GABAergic neurons. Extensive studies in mouse brain also showed high level of expression of neuronatin in PV+ve GABAergic interneurons in the cortex, hippocampus, amygdale and hypothalamus.

LD brain exhibits increased accumulation of neuronatin and loss of PV+ve GABAergic interneurons—The symptoms of LD usually appears early in adolescence. Since neuronatin is widely expressed in developing brain including a subpopulation of GABAergic neurons, we further explored its level and localization in cortical areas of LD brain. To our surprise, we noticed frequent accumulation of neuronatin as insoluble aggregates in cortical areas (Fig.3). Some neurons and their processing also showed very high level of accumulation of neuronatin in comparison to age-matched control brain. Ubiquitin immunostaining also revealed accumulation of insoluble inclusions in the LD brain. Ubiquitin and neuronatin-positive Lafora bodies were strikingly similar in their appearance. Most Lafora bodies were strongly labeled with ubiquitin (Fig.4). In addition, ubiquitin-positive multiple inclusions were also sometimes observed around the perinuclear region (Fig.4). Because neuronatin is expressed in PV+ve GABAergic neurons, we were curious to know the status of these interneurons in LD brain biopsy. We have observed a dramatic loss of the PV+ve GABAergic neurons in the cortical areas of both the LD brain biopsies. It was very hard to find surviving PV+ve GABAergic neurons with processing in the case of LD brain (Fig.5).

Neuronatin is aggregated in response to proteasomal inhibition and its over expression causes increased intracellular Ca^{2+} and apoptosis, which is partially restored by malin—Because neuronatin is accumulated and aggregated in LD brain, we next explored its possible role in neurodegeneration using cultured neuronal cells. Neuronatin was expressed in neuro 2a cells and localized in the membrane and cytosol. Treatment with proteasome inhibitor caused its accumulation and aggregation in the cell indicating that it is rapidly degraded via UPS and its increased accumulation could lead to formation of aggregates (Fig.6A). This finding further supports our observation of neuronatin inclusions in LD brain. Recently, neuronatin is shown to increase the intracellular Ca^{2+} levels by antagonizing ER SERCA2 pump. We have also observed that the over expression or knockdown of neuronatin in neuro 2a cells caused significant increase or decrease in intracellular Ca^{2+} respectively (Fig.6B). Thapsigargin, a non-competitive inhibitor of SERCA pump was used as positive control. Interestingly, co-expression of wild type malin significantly restored the neuronatin-induced increased intracellular Ca^{2+} (Fig.6C). Malin also rescued neuronatin-induced apoptotic cell death (Fig.6D and Supplementary Fig.S2). Although wild type malin had no effect on intracellular Ca^{2+} levels, its LD-associated C26S mutant caused significant increase in intracellular Ca^{2+} and also apoptosis. This is not

surprising because C26S mutant of malin is shown to form aggregates in cell culture and induce apoptosis.

Malin suppresses neuronatin-induced ER stress and proteasomal dysfunction—Increased intracellular free Ca^{2+} as well as accumulation of misfolded proteins is known to generate ER stress in the cell. Since neuronatin increases the cytosolic Ca^{2+}, we tested its effect on the ER stress. As shown in Figure 7, ectopic expression of neuronatin in neuro 2a cells resulted in ER stress in concentration-dependent manner as evident from the increased expression of Grp78, CHOP and IRE-α. Transient co-expression of malin significantly suppressed neuronatin-induced ER stress (Fig.7B). The C26S mutant of malin was also found to generate ER stress and amplified neuronatin-induced ER stress. We have also observed proteasomal dysfunction in neuronatin over expressed cells as shown from the decrease in proteasome activity and increased accumulation of ubiquitinated proteins (Fig.8A and B). Neuronatin over expression also caused increased accumulation of d1EGFP, a model substrate of proteasome with half-life of about 1 h. (Fig.8C and D). Co-expression of malin along with neuronatin partially restored neuronatin-induced proteasomal inhibition (Fig 8E). The C26S mutant of malin also inhibited cellular proteasomal function that was enhanced further in the presence of neuronatin. These *in vitro* studies indicate that increased accumulation of neuronatin is toxic to the neuron, which is mediated by increased intracellular free Ca^{2+} followed by ER stress and proteasomal dysfunction. LD-associated mutant malin also could be implicated in the ER stress generation, proteasomal dysfunction and neurodegeneration.

Discussion

We had demonstrated earlier that malin interacts with neuronatin and promotes its degradation through proteasome (39). Here, we provide substantial evidence that indicates crucial role of neuronatin in LD pathogenesis. First, we show that the level of neuronatin is significantly increased in the sweat gland of skin of LD patients having mutations not only in malin but also in laforin in contrast to control samples. Neuronatin level is also increased and often aggregated and sometimes associated with Lafora bodies in cortical neurons of LD brain biopsy samples. Ectopic expression of neuronatin in the neuronal cell leads to increase in intracellular Ca^{2+} and induction of apoptotic cell death. Increased accumulation of neuronatin in the skin samples of either malin or laforin mutant patients imply that these two protein complex are involved in the turnover of neuronatin. Laforin and malin are shown to function as a complex (14,45,46) and in the malin knockout mice, laforin is increased in insoluble fraction (21,22) and therefore might be biologically inactive. Similarly, in the absence of laforin, malin also could be nonfunctional because malin is shown to be an aggregation prone protein and can be stabilized upon binding with laforin (40).

Neuronatin is highly expressed in neonatal brain and possibly involved in neural induction and neuronal differentiation during brain development (27,38). In the adult mice, it is also found to be selectively expressed in various limbic structures (31) of brain and several non-neural tissues including skin (33,34). Existing literature suggests the involvement of neuronatin in the regulation of glycogen and lipid metabolism and its mutation is associated with obesity (31,32,37,39). The primary and secondary structure of neuronatin is also strikingly similar with phospholamban (an ER-resident Ca^{2+} regulator found in cardiac muscle) and recent reports have demonstrated that it is indeed involved in increasing the intracellular Ca^{2+} by antagonizing SERCA2 pump in the ER (27,38). We have also detected significant increase in intracellular Ca^{2+} in neuronatin transfected neuroblastoma cells. Since malin regulates neuronatin level, we speculate that malin might

also be associated with certain aspects of brain development and regulation of metabolism.

Although the biological role of neuronatin in the skin is not clear, it is possible that high levels of neuronatin in LD skin might be involved with abnormal function of sweat gland and Lafora body formation. In the developing LD brain, neuronatin level is increased and might be progressively accumulating as an insoluble aggregates in post mitotic neurons. Neuronatin seems to be an unfolded and aggregate prone protein that is recognized and rapidly cleared by UPS. Blockade of cellular proteasome function leads to its aberrant accumulation and aggregation. Therefore, lack of function of malin-laforin complex could result in inefficient clearance of unfolded neuronatin leading to its accumulation and aggregation particularly in the neurons. Increased accumulation of neuronatin or its aggregates could potentially induce neurodegeneration by increasing intracellular Ca^{2+} overload followed by ER and proteasomal stress. We have also shown here that over expression of malin partially recovered neuronatin-induced ER stress and proteasomal dysfunction and rescued the neuronatin-induced cell death. Our findings are consistent with other reports suggesting a role for malin-laforin complex in the clearance of misfolded proteins and involvement of ER stress in LD pathogenesis (46,47).

Interestingly, neuronatin is highly expressed in PV+ve GABAergic interneuron and these inhibitory interneurons dramatically degenerated in LD brain. PV is a Ca^{2+} buffering protein in cytosol and expression of neuronatin in PV-containing GABAergic interneurons indicate that neuronatin might be playing a pivotal role in Ca^{2+}-mediated GABAergic neurotransmission and signaling pathways. Excessive accumulation of neuronatin could potentially lead to the degeneration of these inhibitory interneurons in LD brain by disturbing Ca^{2+} homeostasis and inducing ER stress. Our findings are very similar with a recent report that demonstrated progressive degeneration of PV+ve GABAergic interneuron in the hippocampus of malin knockout mice (23). The loss of PV+ve inhibitory interneurons in LD brain could potentially explain rapidly progressing seizures and myoclonus in this disease.

Although the Lafora body is one of the common pathological hallmarks of LD, its involvement in disease pathogenesis is not clearly understood. In laforin deficient mice, degenerating neurons sometimes lacked Lafora bodies (24), while depletion of protein targeting to glycogen (PTG) in the same mice results in disappearance of Lafora bodies and rescue of neurodegeneration and seizures (25). Emerging literature now indicate that the defect in UPS and autophagy might be causative for the evolution of LD (17,18,26,46,47). Lafora bodies are found to be associated with various components of UPS and autophagy and could potentially induce the defect in these intracellular protein degradation pathways (17,26). Accumulation of unfolded neuronatin along with LD-associated malin or laforin mutant proteins in neurons could also potentially disturb protein quality control system. Taken together, our finding suggests that the neuronatin-induced aberrant Ca^{2+} signaling and ER stress might be an important contributor in LD pathogenesis. We also indicate that LD can now join to the list of neurodegenerative disorders involving accumulation of misfolded proteins.

References

1. Acharya, J. N., Satishchandra, P., Asha, T., and Shankar, S. K. (1993) *Epilepsia* **34**, 476-487
2. Singh, S., and Ganesh, S. (2009) *Hum Mutat* **30**, 715-723
3. Delgado-Escueta, A. V. (2007) *Curr Neurol Neurosci Rep* **7**, 428-433
4. Minassian, B. A. (2001) *Pediatr Neurol* **25**, 21-29
5. Ganesh, S., Puri, R., Singh, S., Mittal, S., and Dubey, D. (2006) *J Hum Genet* **51**, 1-8
6. Carpenter, S., and Karpati, G. (1981) *Neurology* **31**, 1564-1568
7. Chan, E. M., Young, E. J., Ianzano, L., Munteanu, I., Zhao, X., Christopoulos, C. C., Avanzini, G., Elia, M., Ackerley, C. A., Jovic, N. J., Bohlega, S., Andermann, E., Rouleau, G. A., Delgado-Escueta, A. V., Minassian, B. A., and Scherer, S. W. (2003) *Nat Genet* **35**, 125-127
8. Chan, E. M., Omer, S., Ahmed, M., Bridges, L. R., Bennett, C., Scherer, S. W., and Minassian, B. A. (2004) *Neurology* **63**, 565-567
9. Minassian, B. A., Lee, J. R., Herbrick, J. A., Huizenga, J., Soder, S., Mungall, A. J., Dunham, I., Gardner, R., Fong, C. Y., Carpenter, S., Jardim, L., Satishchandra, P., Andermann, E., Snead, O. C., 3rd, Lopes-Cendes, I., Tsui, L. C., Delgado-Escueta, A. V., Rouleau, G. A., and Scherer, S. W. (1998) *Nat Genet* **20**, 171-174
10. Singh, S., Sethi, I., Francheschetti, S., Riggio, C., Avanzini, G., Yamakawa, K., Delgado-Escueta, A. V., and Ganesh, S. (2006) *J Med Genet* **43**, e48
11. Lohi, H., Ianzano, L., Zhao, X. C., Chan, E. M., Turnbull, J., Scherer, S. W., Ackerley, C. A., and Minassian, B. A. (2005) *Human molecular genetics* **14**, 2727-2736
12. Solaz-Fuster, M. C., Gimeno-Alcaniz, J. V., Ros, S., Fernandez-Sanchez, M. E., Garcia-Fojeda, B., Criado Garcia, O., Vilchez, D., Dominguez, J., Garcia-Rocha, M., Sanchez-Piris, M., Aguado, C., Knecht, E., Serratosa, J., Guinovart, J. J., Sanz, P., and Rodriguez de Cordoba, S. (2008) *Human molecular genetics* **17**, 667-678
13. Worby, C. A., Gentry, M. S., and Dixon, J. E. (2008) *The Journal of biological chemistry* **283**, 4069-4076
14. Vilchez, D., Ros, S., Cifuentes, D., Pujadas, L., Valles, J., Garcia-Fojeda, B., Criado-Garcia, O., Fernandez-Sanchez, E., Medrano-Fernandez, I., Dominguez, J., Garcia-Rocha, M., Soriano, E., Rodriguez de Cordoba, S., and Guinovart, J. J. (2007) *Nat Neurosci* **10**, 1407-1413
15. Cheng, A., Zhang, M., Gentry, M. S., Worby, C. A., Dixon, J. E., and Saltiel, A. R. (2007) *Genes Dev* **21**, 2399-2409
16. Aguado, C., Sarkar, S., Korolchuk, V. I., Criado, O., Vernia, S., Boya, P., Sanz, P., de Cordoba, S. R., Knecht, E., and Rubinsztein, D. C. (2010) *Human molecular genetics* **19**, 2867-2876
17. Puri, R., Suzuki, T., Yamakawa, K., and Ganesh, S. (2011) *Human molecular genetics*
18. Criado, O., Aguado, C., Gayarre, J., Duran-Trio, L., Garcia-Cabrero, A. M., Vernia, S., San Millan, B., Heredia, M., Roma-Mateo, C., Mouron, S., Juana-Lopez, L., Dominguez, M., Navarro, C., Serratosa, J. M., Sanchez, M., Sanz, P., Bovolenta, P., Knecht, E., and Rodriguez de Cordoba, S. (2011) *Human molecular genetics*
19. Wang, Y., Liu, Y., Wu, C., Zhang, H., Zheng, X., Zheng, Z., Geiger, T. L., Nuovo, G. J., Liu, Y., and Zheng, P. (2006) *Cancer Cell* **10**, 179-190
20. Sharma, J., Mulherkar, S., Mukherjee, D., and Jana, N. R. (2012) *The Journal of biological chemistry*
21. DePaoli-Roach, A. A., Tagliabracci, V. S., Segvich, D. M., Meyer, C. M., Irimia, J. M., and Roach, P. J. (2010) *The Journal of biological chemistry* **285**, 25372-25381

22. Turnbull, J., Wang, P., Girard, J. M., Ruggieri, A., Wang, T. J., Draginov, A. G., Kameka, A. P., Pencea, N., Zhao, X., Ackerley, C. A., and Minassian, B. A. (2010) *Annals of neurology* **68**, 925-933
23. Valles-Ortega, J., Duran, J., Garcia-Rocha, M., Bosch, C., Saez, I., Pujadas, L., Serafin, A., Canas, X., Soriano, E., Delgado-Garcia, J. M., Gruart, A., and Guinovart, J. J. (2011) *EMBO molecular medicine* **3**, 667-681
24. Ganesh, S., Delgado-Escueta, A. V., Sakamoto, T., Avila, M. R., Machado-Salas, J., Hoshii, Y., Akagi, T., Gomi, H., Suzuki, T., Amano, K., Agarwala, K. L., Hasegawa, Y., Bai, D. S., Ishihara, T., Hashikawa, T., Itohara, S., Cornford, E. M., Niki, H., and Yamakawa, K. (2002) *Human molecular genetics* **11**, 1251-1262
25. Turnbull, J., DePaoli-Roach, A. A., Zhao, X., Cortez, M. A., Pencea, N., Tiberia, E., Piliguian, M., Roach, P. J., Wang, P., Ackerley, C. A., and Minassian, B. A. (2011) *PLoS genetics* **7**, e1002037
26. Rao, S. N., Maity, R., Sharma, J., Dey, P., Shankar, S. K., Satishchandra, P., and Jana, N. R. (2010) *Human molecular genetics* **19**, 4726-4734
27. Dou, D., and Joseph, R. (1996) *Brain Res* **723**, 8-22
28. Joseph, R., Dou, D., and Tsang, W. (1994) *Biochem Biophys Res Commun* **201**, 1227-1234
29. Joseph, R., Dou, D., and Tsang, W. (1995) *Brain Res* **690**, 92-98
30. Dou, D., and Joseph, R. (1996) *Genomics* **33**, 292-297
31. Vrang, N., Meyre, D., Froguel, P., Jelsing, J., Tang-Christensen, M., Vatin, V., Mikkelsen, J. D., Thirstrup, K., Larsen, L. K., Cullberg, K. B., Fahrenkrug, J., Jacobson, P., Sjostrom, L., Carlsson, L. M., Liu, Y., Liu, X., Deng, H. W., and Larsen, P. J. (2010) *Obesity (Silver Spring)* **18**, 1289-1296
32. Mzhavia, N., Yu, S., Ikeda, S., Chu, T. T., Goldberg, I., and Dansky, H. M. (2008) *Diabetes* **57**, 2774-2783
33. Arava, Y., Adamsky, K., Ezerzer, C., Ablamunits, V., and Walker, M. D. (1999) *Diabetes* **48**, 552-556
34. Dugu, L., Takahara, M., Tsuji, G., Iwashita, Y., Liu, X., and Furue, M. (2010) *The Journal of dermatology* **37**, 846-848
35. Chu, K., and Tsai, M. J. (2005) *Diabetes* **54**, 1064-1073
36. Suh, Y. H., Kim, W. H., Moon, C., Hong, Y. H., Eun, S. Y., Lim, J. H., Choi, J. S., Song, J., and Jung, M. H. (2005) *Biochem Biophys Res Commun* **337**, 481-489
37. Joe, M. K., Lee, H. J., Suh, Y. H., Han, K. L., Lim, J. H., Song, J., Seong, J. K., and Jung, M. H. (2008) *Cell Signal* **20**, 907-915
38. Lin, H. H., Bell, E., Uwanogho, D., Perfect, L. W., Noristani, H., Bates, T. J., Snetkov, V., Price, J., and Sun, Y. M. (2010) *Stem cells (Dayton, Ohio)* **28**, 1950-1960
39. Sharma, J., Rao, S. N., Shankar, S. K., Satishchandra, P., and Jana, N. R. (2011) *Neurobiology of disease* **44**, 133-141
40. Rao, S. N., Sharma, J., Maity, R., and Jana, N. R. (2010) *The Journal of biological chemistry* **285**, 1404-1413
41. Jana, N. R., Dikshit, P., Goswami, A., and Nukina, N. (2004) *The Journal of biological chemistry* **279**, 11680-11685
42. Mishra, A., Godavarthi, S. K., Maheshwari, M., Goswami, A., and Jana, N. R. (2009) *The Journal of biological chemistry* **284**, 10537-10545
43. Grynkiewicz, G., Poenie, M., and Tsien, R. Y. (1985) *The Journal of biological chemistry* **260**, 3440-3450

44. Sinha, S., Satishchandra, P., Gayathri, N., Yasha, T. C., and Shankar, S. K. (2007) *J Neurol Sci* **252**, 16-23
45. Gentry, M. S., Worby, C. A., and Dixon, J. E. (2005) *Proc Natl Acad Sci U S A* **102**, 8501-8506
46. Garyali, P., Siwach, P., Singh, P. K., Puri, R., Mittal, S., Sengupta, S., Parihar, R., and Ganesh, S. (2009) *Human molecular genetics* **18**, 688-700
47. Vernia, S., Rubio, T., Heredia, M., Rodriguez de Cordoba, S., and Sanz, P. (2009) *PLoS One* **4**, e5907

Acknowledgements—This work was supported in part by a core grant from the Department of Biotechnology to National Brain Research Centre, Government of India and also an extramural grant from the Department of Biotechnology (BT/PR13590/MED/30/286/2009). J. S. was supported by research fellowship from Department of Biotechnology, Government of India.

Footnote—First two authors are contributed equally to this work.

Figure legends

Figure 1. Neuronatin level is increased in axillary skin biopsy samples collected from malin and laforin mutant LD patients. Skin biopsy samples obtained from three controls (sample number 1718, 1762 and 1848) and three LD patients (one laforin and two malin mutants) were stained immunohistochemically using neuronatin antibody. Each LD skin samples showed PAS-positive Lafora bodies. Hsc70/Hsp70 antibody was used as positive control that detects Lafora bodies. In negative control (NC), sample was processed without primary antibody. Scale bar; 20 μm.

Figure 2. Age-dependent changes in the expression and localization of neuronatin in human brain. A) Brain sections of different ages were immunohistochemically stained with neuronatin antibody. Arrow indicates the cell expressing high level of neuronatin and arrowhead pointed the localization of neuronatin in neuritic puncta. Scale bar; 40 μm. B) Double immunofluorescence staining showing localization of neuronatin with PV+ve GABAergic interneurons. Scale bar; 20 μm. Nuclei were counterstained with DAPI. FITC-conjugated secondary antibody was used to detect PV and Alexa Fluor 594-labeled secondary was used to recognize neuronatin.

Figure 3. Immunohistochemical staining of neuronatin and ubiquitin in control (15 years old) and two different LD brain biopsy samples (LD1 and LD2 of 17 and 23 years old respectively). Lower panel of neuronatin staining shows higher magnification images. Arrow indicates neuronatin or ubiquitin-positive inclusions. Arrowhead pointed the cell or neurites exhibiting high level of neuronatin in LD brain. PAS staining was conducted to confirm the presence of Lafora bodies (indicated by arrow) in LD brain samples. In negative control (NC), LD brain section was processed without neuronatin antibody. Scale bars; 40 μm in smaller magnification images and 20 μm in higher magnification images. Bottom panel shows higher magnification images of localization of neuronatin or ubiquitin into Lafora bodies.

Figure 4. A) Immunohistochemical staining of ubiquitin in LD brain biopsy samples showing ubiquitin-positive perinuclear aggregates. B) Co-localization of ubiquitin with PAS-positive Lafora body.

Figure 5. Immunohistochemical staining PV+ve GABAergic interneurons in control and LD brain biopsy samples. Arrow indicate PV+ve neurons that are degenerated in LD brain samples. Scale bar; 20 μm.

Figure 6. Neuronatin is degraded by proteasome and it's over expression leads to increased intracellular Ca^{2+} and apoptosis that can be suppressed by malin. A) Neuro 2a cells were plated onto 6-well tissue cultured plates or two-well chamber slides and on the following day cells were treated with MG132 (10 μM for 6 h) and processed for immunofluorescence staining or immunoblot analysis using neuronatin antibody. Scale bar; 20 μm. B) Neuro 2a cells were plated onto 6-well tissue cultured plates and 24 h later cells were transiently transfected with either neuronatin β plasmid (Nnatβ OE, 2 μg/well) or neuronatin siRNA (30 pmol/well) for 36 h. In some experiment, cells were treated with thapsigargin (1 μM for 12 h). The cells were then processed for either measurement of intracellular Ca^{2+} or immunoblot analysis using neuronatin, myc (to detect over expressed neuronatin) and GAPDH antibodies. C) Cells were transfected with plasmid encoding empty pcDNA3.1 (control) or neuronatin β plasmid alone or along with wild type or C26S mutant of malin (2 μg of each plasmid/well of 6-well plate). Thirty-six hours of post transfection, cells were subjected to the analysis of intracellular Ca^{2+} levels. In B and C, values are mean ± SD of three independent experiments each performed triplicate. *$p<0.01$ in comparison with control. **$p<0.01$ compared to neuronatin transfected group. D) Neuronatin-induced

cell death is protected by malin and aggravated by LD-associated C26S mutant of malin. Cells were transfected with LacZ or neuronatin β plasmid independently or along with malin plasmids as in C for 72 h. Cells were differentiated with dbcAMP (5 mM for 48 h) and then processed for immunofluorescence staining to identify neuronatin or neuronatin and malin transfected cells. Nuclei were stained with DAPI to identify the apoptotic cell (fragmented nuclei, see Supplementary Fig.S2). Values are mean ± SD of three independent experiments with minimum of 200 transfected cells counted for each experiment. *p<0.001 in comparison with LacZ transfected control and **p<0.01 compared to neuronatin transfected group.

Figure 7. Neuronatin induces ER stress, which is suppressed by malin and enhanced by C26S mutant of malin. A) Neuro 2a cells were transfected with different concentrations of neuronatin plasmid for 48 h. Cells were treated with dbcAMP (5 mM) for 24 h before collection and then subjected to immunoblot analysis using various antibodies as indicated in the figure. Tunicamycin (Tuni, 25 μg/ml) was treated for 6 h. Band intensities of Grp78, IRE-α and CHOP were quantified using NIH Image analysis software, normalized against β-tubulin and expressed as fold change. B) Cells were transfected with plasmid encoding neuronatin or malin independently or together for 48 h, treated with dbcAMP as in A and then processed for immunoblotting using various antibodies shown in the figure. Grp78 and CHOP blots were quantified, normalized against β-tubulin and expressed as fold change. Values are mean ± SD of four different experiments. *p<0.05 and **p<0.01 compared to respective empty pcDNA3.1 transfected group and ***p<0.01 compared to neuronatin transfected group.

Figure 8. Neuronatin-induced proteasomal dysfunction is partially recovered by malin. A, B) Neuro 2a cells were transfected with different concentrations of plasmid encoding neuronatin and differentiated as described in Figure 6A. Forty-eight hours of post transfection, cells were either processed for proteasome activity assays (A) or immunoblot analysis using ubiquitin, myc (to detect neuronatin β) and GAPDH antibodies (B). Values are mean ± SD of three independent experiments each performed triplicates. *p<0.01 in comparison with control. C) Cells were transiently transfected with plasmid encoding pd1EGFP alone or along with neuronatin β for 48 h and the collected cells were then processed for immunoblotting using antibody against GFP. D) The band intensities of d1EGFP from three independent experiments were quantified using NIH Image analysis software. Proteasome inhibitor MG132 (20 μM for 6 h) was used as positive control. *p<0.001 in comparison with control. E) Cells were transfected with various plasmids and differentiated as described in Figure 6B. Cells were collected and subjected to proteasome activity assay. Values are mean ± SD of three different experiments each performed in triplicates. *p<0.01 compared to empty pcDNA3.1 transfected group (control) and **p<0.01 compared to neuronatin transfected group.

Fig.1

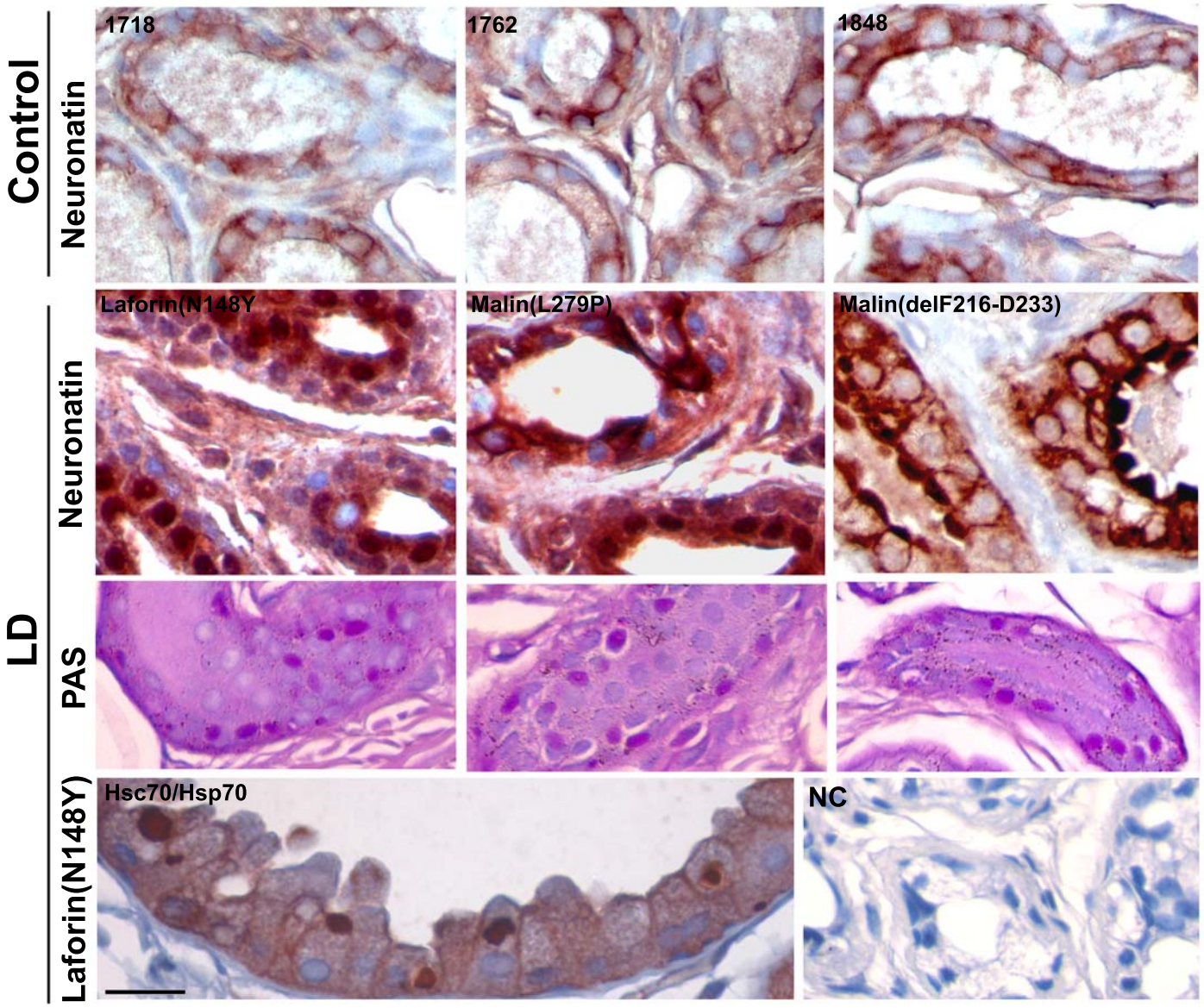
Control
Neuronatin
1718
1762
1848
LD
Neuronatin
Laforin(N148Y
Malin(L279P)
Malin(delF216-D233)
PAS
Laforin(N148Y)
Hsc70/Hsp70
NC

Fig.2

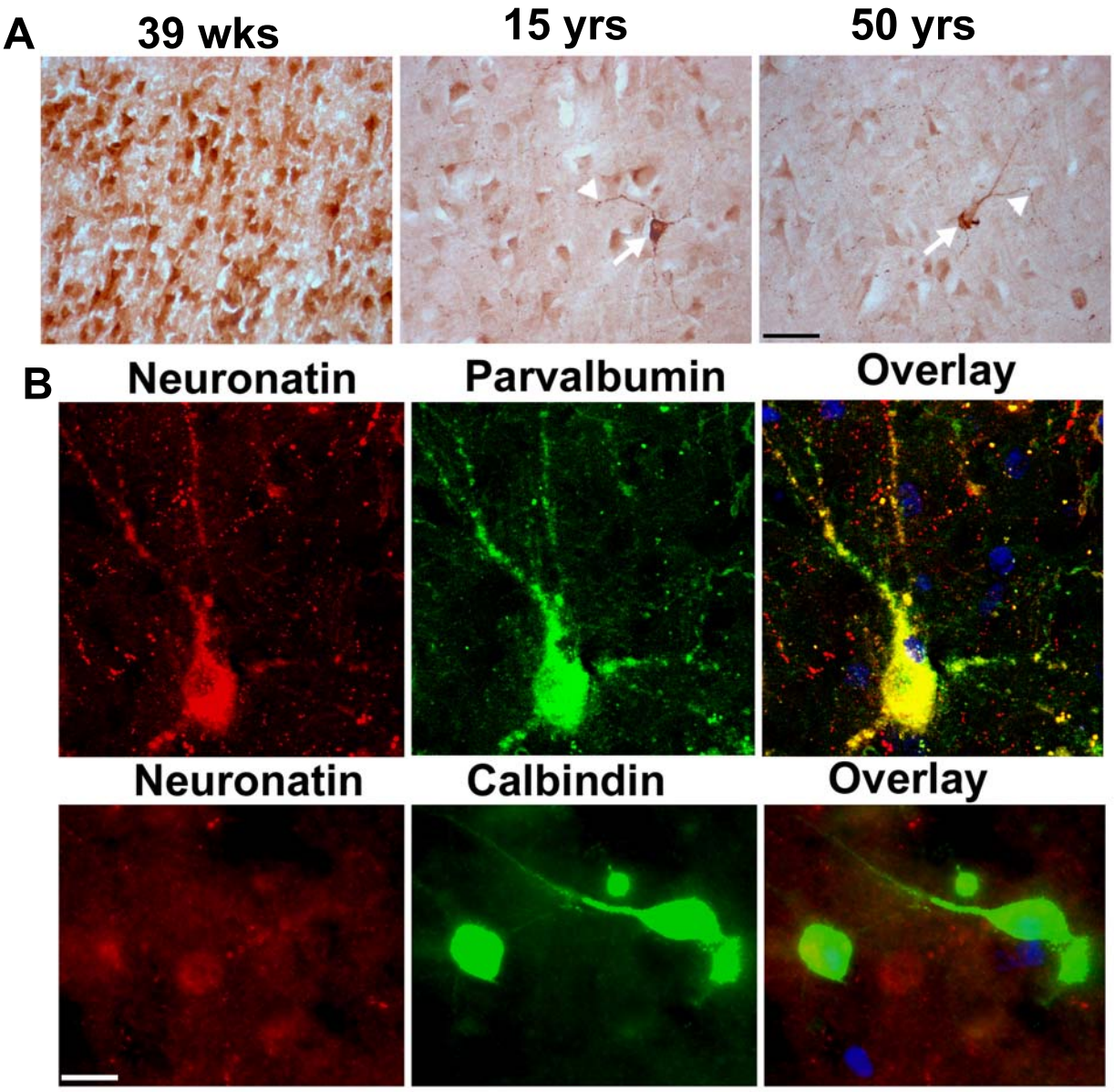
A
39 wks
15 yrs
50 yrs
B
Neuronatin
Parvalbumin
Overlay
Neuronatin
Calbindin
Overlay

Fig.3

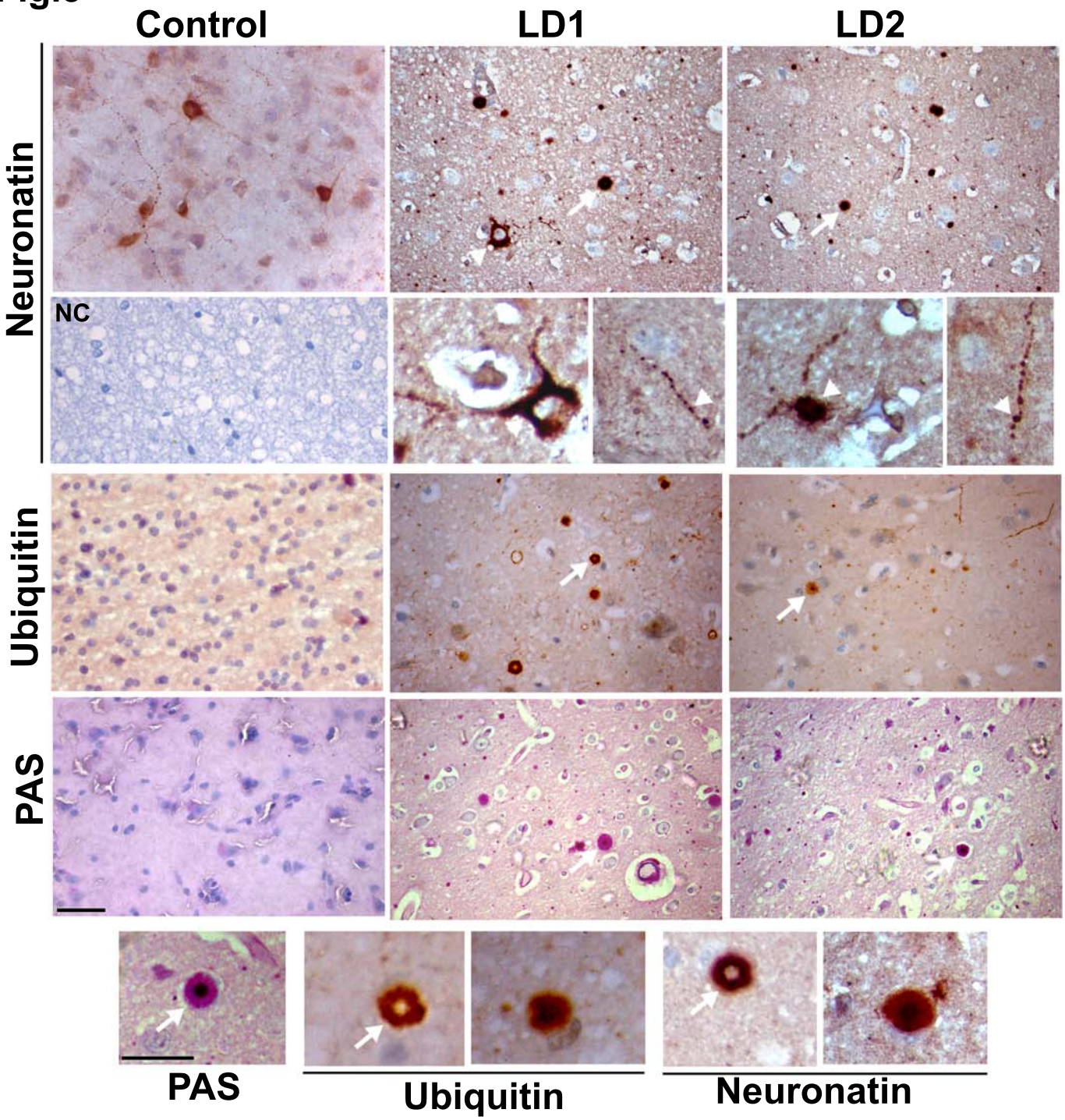
Control
LD1
LD2
Neuronatin
NC
Ubiquitin
PAS
PAS
Ubiquitin
Neuronatin

Fig.4

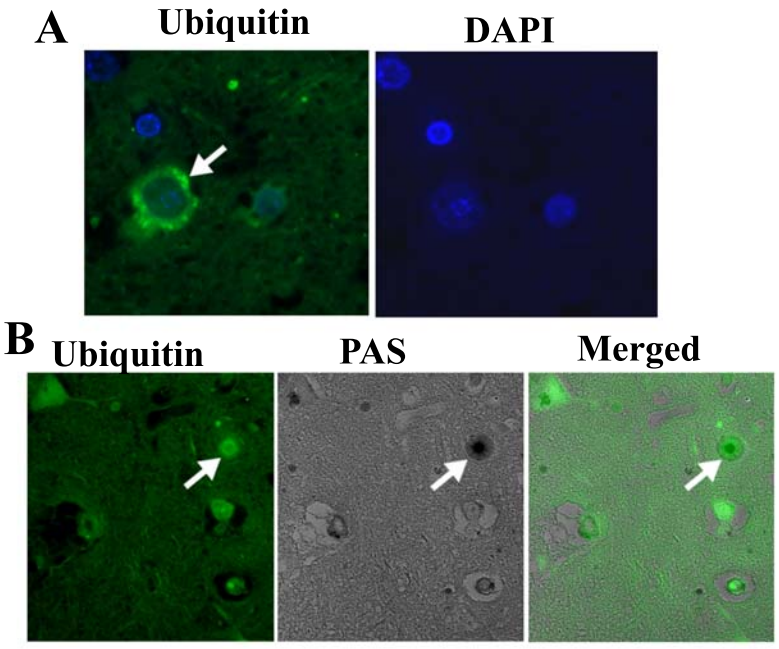

Fig.5

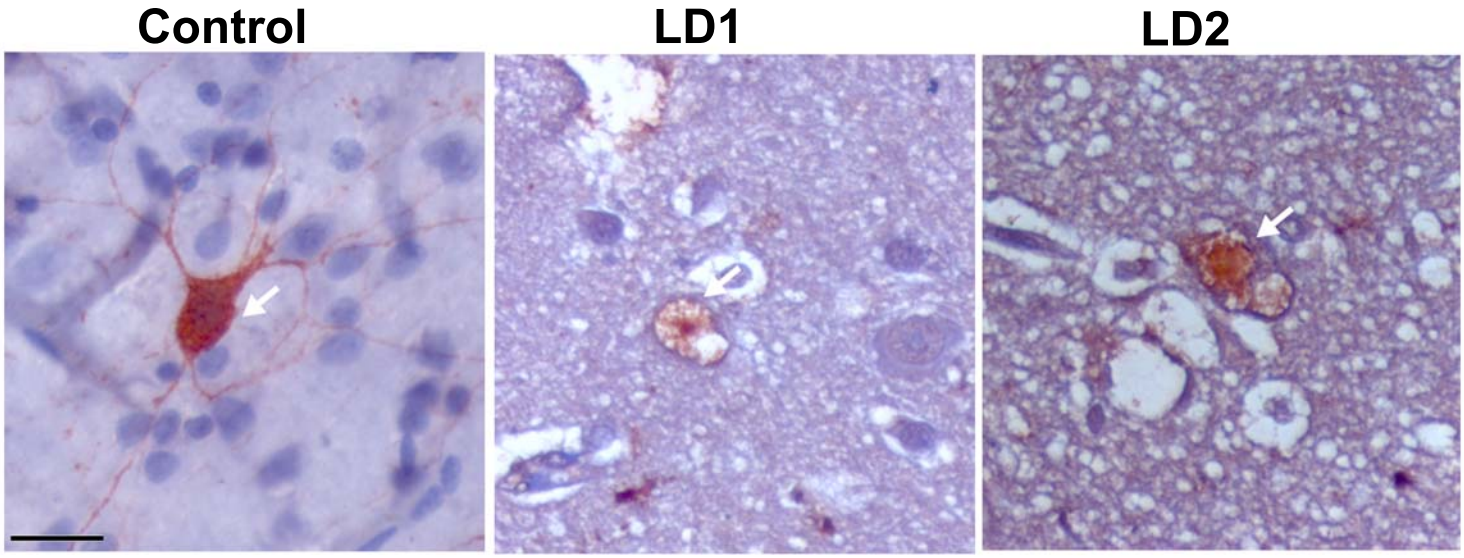

Fig.6

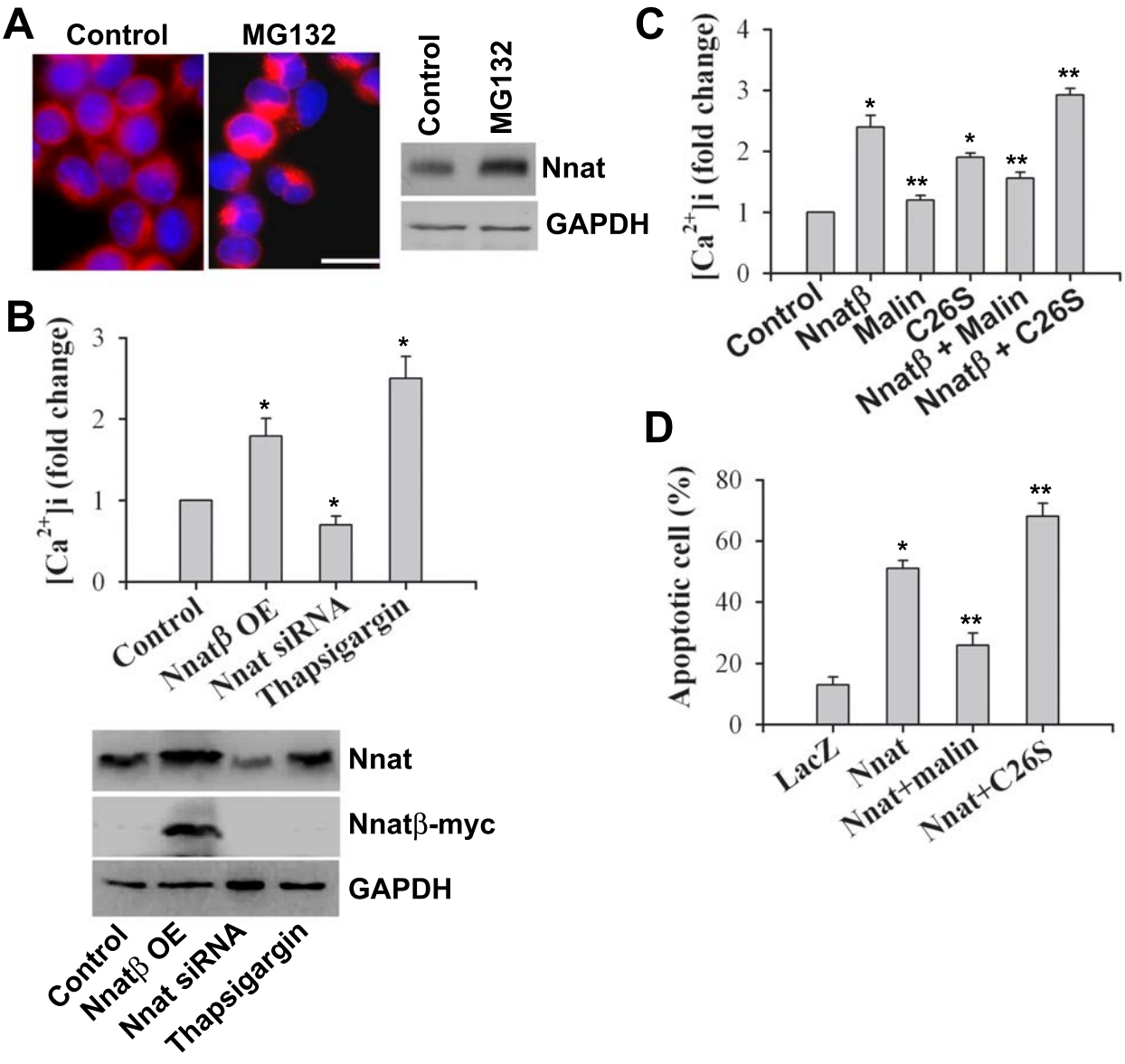
A
Control
MG132
Control
MG132
Nnat
GAPDH
B
[Ca2+]i (fold change)
Control
Nnatβ OE
Nnat siRNA
Thapsigargin
Nnat
Nnatβ-myc
GAPDH
Control
Nnatβ OE
Nnat siRNA
Thapsigargin
C
[Ca2+]i (fold change)
Control
Nnatβ
Malin
C26S
Nnatβ + Malin
Nnatβ + C26S
D
Apoptotic cell (%)
LacZ
Nnat
Nnat+malin
Nnat+C26S

Fig.7

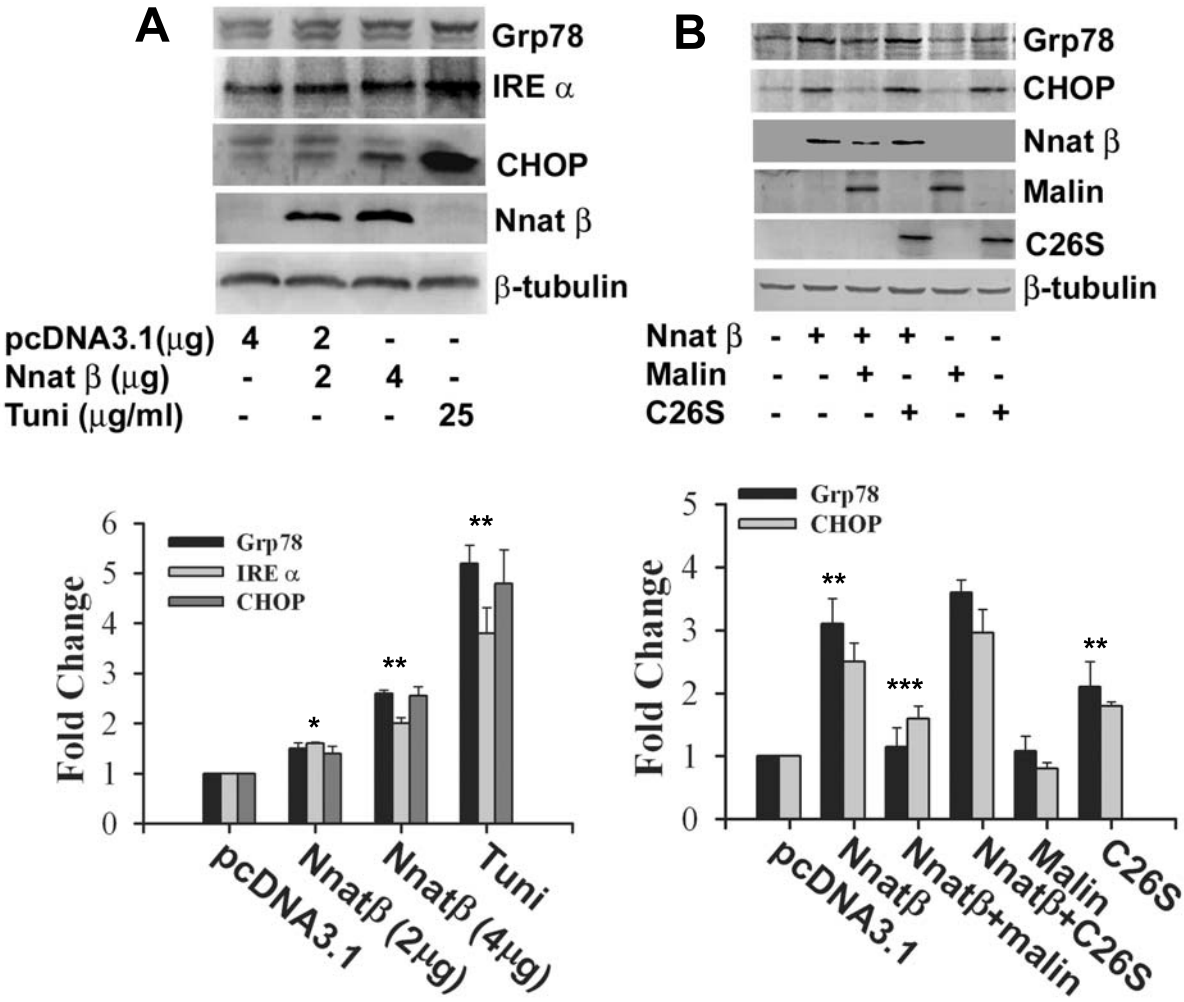
A
Grp78
IRE α
CHOP
Nnat β
β-tubulin
pcDNA3.1(μg) 4 2 - -
Nnat β (μg) - 2 4 -
Tuni (μg/ml) - - - 25
B
Grp78
CHOP
Nnat β
Malin
C26S
β-tubulin
Nnat β - + + + - -
Malin - - + - + -
C26S - - - + - +
Fold Change
Grp78
IRE α
CHOP
pcDNA3.1
Nnatβ (2μg)
Nnatβ (4μg)
Tuni
Fold Change
Grp78
CHOP
pcDNA3.1
Nnatβ
Nnatβ+malin
Nnatβ+C26S
Malin
C26S

Fig.8

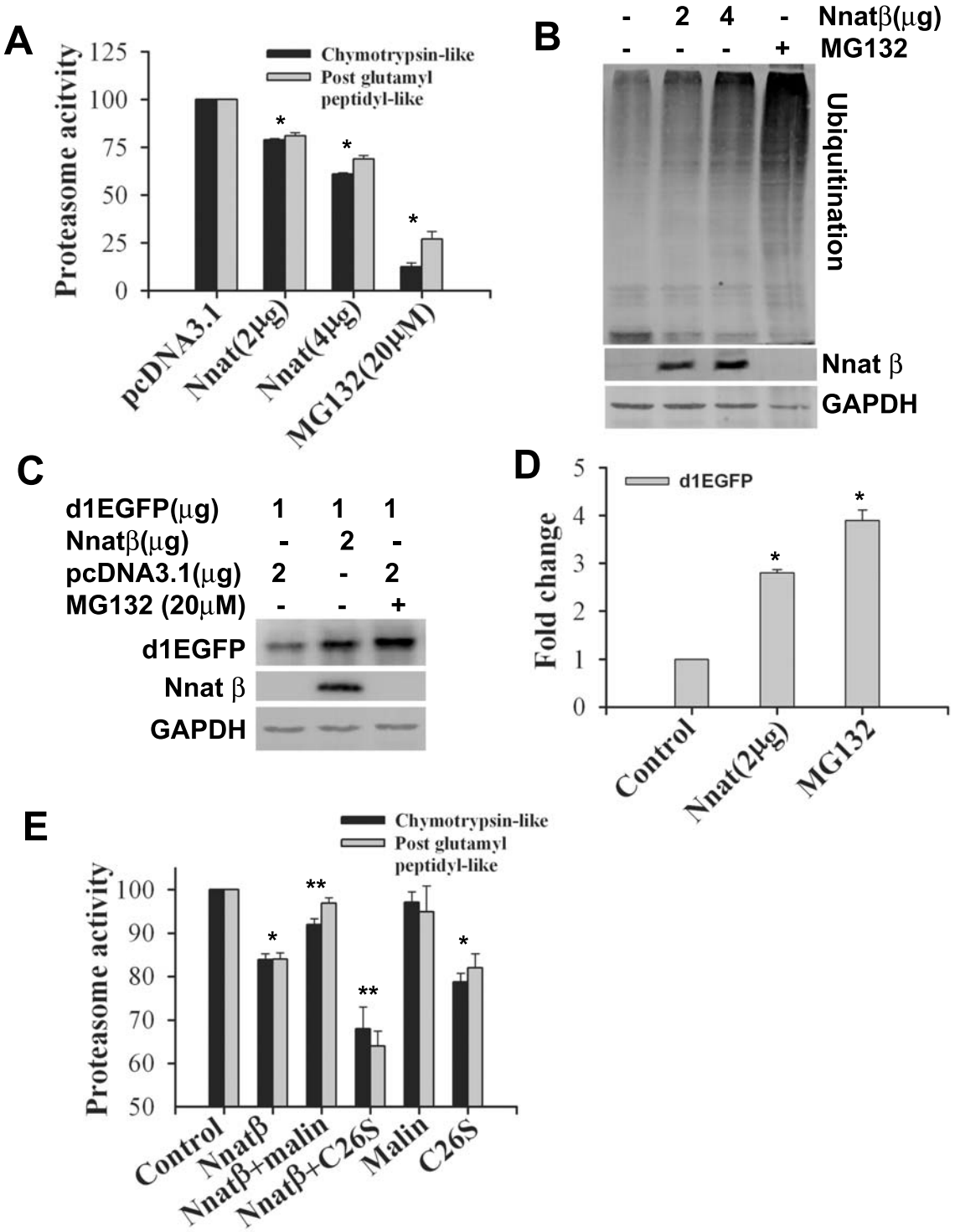
A
Proteasome acitvity
125
100
75
50
25
0
Chymotrypsin-like
Post glutamyl peptidyl-like
*
*
*
pcDNA3.1
Nnat(2μg)
Nnat(4μg)
MG132(20μM)
B
- 2 4 - Nnatβ(μg)
- - - + MG132
Ubiquitination
Nnat β
GAPDH
C
d1EGFP(μg) 1 1 1
Nnatβ(μg) - 2 -
pcDNA3.1(μg) 2 - 2
MG132 (20μM) - - +
d1EGFP
Nnat β
GAPDH
D
Fold change
5
4
3
2
1
0
d1EGFP
*
*
Control
Nnat(2μg)
MG132
E
Proteasome activity
100
90
80
70
60
50
Chymotrypsin-like
Post glutamyl peptidyl-like
*
**
**
*
Control
Nnatβ
Nnatβ+malin
Nnatβ+C26S
Malin
C26S